EXPERIMENTAL INVESTIGATION OF SEMI-RIGID STEEL BEAM-COLUMN CONNECTIONS

J. B. Radziminski (I)
J. H. Bradburn (II)
Presenting Author: J. B. Radziminski

SUMMARY

This paper presents the results of an experimental study of the performance of semi-rigid steel beam-to-column connections under static and cyclic loadings. From the static tests, the geometric parameters which most significantly affect the moment-rotation behavior of the connections have been evaluated. Under controlled displacement cyclic loadings, the connections exhibited ductile behavior, with generally stable moment-rotation hysteresis loops evident at each displacement amplitude. The cyclic tests further demonstrated that the effectiveness of these connections, under seismic loading, may be limited by low cycle fatigue of the connection elements.

INTRODUCTION

The satisfactory performance of ductile moment-resisting steel frame building structures in an earthquake environment is dependent upon the ability of the beam-column connections to provide the rigid frame behavior and energy absorption capacity necessary to withstand the seismically induced lateral forces. Considerable experimental data has been generated on the moment-rotation behavior of rigid connections (e.g., Refs. 1, 2), which have demonstrated that such connections provide adequate strength and ductility to insure the required performance of the structural system. Recently, studies have been reported (e.g., Refs. 1, 3, 4) which consider the effect of connection flexibility on the performance of building frames. The analytical predictions of frame behavior are typically based on assumed non-linear mathematical models of the beam-column connections. However, there is a need for additional experimental data to substantiate the appropriateness of the mathematical models used to describe semi-rigid connections, particularly those utilizing high-strength bolted connection elements. In the present study, the moment-rotation behavior of connections consisting of bolted top and seat beam flange angles, together with standard bolted web angles, has been investigated. The objectives of the study have been to experimentally determine the effect of varying the connection stiffness on the static response of the connections, and to obtain a measure of their hysteretic energy absorption under cyclic loadings.

EXPERIMENTAL INVESTIGATION

A pair of beam sections attached to a centrally positioned stub column comprised the test members. The connection elements consisted of top and seat

(I) Professor of Civil Engineering, University of South Carolina, Columbia, S.C., USA

(II) Associate Professor of Civil Engineering, University of South Carolina, Columbia, S.C., USA

angles bolted to the flanges of the beams and supporting stub column, together with double web angles bolted to the beam web and column flange. The top and seat angles were the same for a given test, and the web angles were centered on the beam. ASTM A36 steel was used for the members and connection elements; the fasteners were 3/4-in. diameter, ASTM A325 high-strength bolts. Bolting was accomplished with an air wrench using the turn-of-the-nut method; A325 flat hardened washers were used under the turned elements.

Two beam sizes, W14x38 and W8x21, were used in the test program. For the 14 in. sections, the overall beam length was 20 ft., and for the 8 in. sections, 12 ft., so that the span-to-depth ratios were slightly less than 20 in each case. The stub column for the W14x38 beams was a W12x96 section, and a W12x58 column section was used with the W8x21 beams. Heavy column sections were selected to eliminate column panel zone distress as a contributing behavioral factor, thereby confining the moment-rotation interaction to the connection elements. The details of the connections used to frame the W14x38 and W8x21 beams are shown in Figs. 1 and 2, respectively. The general configurations of the test members are shown in Fig. 3.

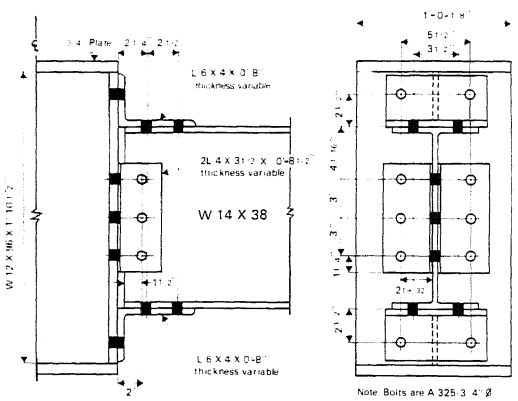

FIG. 1 DETAILS OF CONNECTION FOR W14X38 BEAM

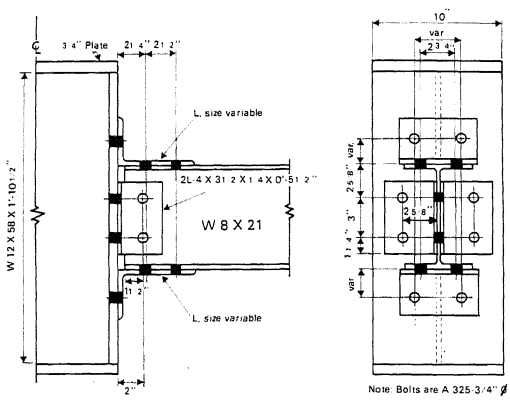

FIG. 2 DETAILS OF CONNECTION FOR W8X21 BEAM

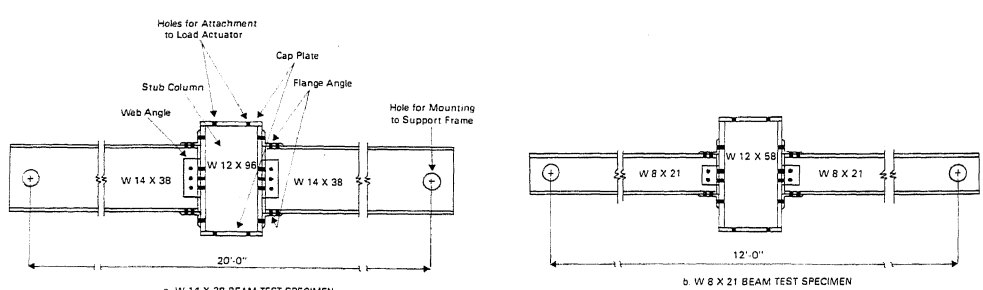

FIG. 3 GENERAL CONFIGURATIONS OF TEST SPECIMENS

A pair of duplicate specimens was tested simultaneously by framing the beams into the central stub column. The beam sections were supported at the ends by roller-type seats located at the beam mid-depth, and designed to allow longitudinal movement, so that no direct axial forces would be introduced as a specimen deflected. Roller guides were used to insure vertical movement of the stub column. A 55 kip, hydraulically actuated ram was used to apply load

to the test members through the stub column. Local monitoring of the load and actuator displacement was accomplished through an x-y plotter. In addition, the data from various displacement measuring devices were transferred directly to a computer for subsequent display and analysis.

For both the static and the cyclic tests, the controlled input variables were the rate and magnitude of actuator displacement and, correspondingly, the displacement of the stub column. For the static test series, a test was concluded when the displacement reached 4 in. for the 20-ft. long W14x38 beam specimens, and 3 in. for the 12-ft. long W8x21 beams. For the cyclic studies, an initial range of actuator displacement of 0.4 in. was selected, intended to provide a hysteresis loop representing minimal non-linear response. A series of 12-15 complete reversal displacement cycles was usually imposed, followed by an increase in the displacement range to 0.8 in. The process was then repeated, with each series of constant amplitude cycles being followed by a 0.4-in. increase in displacement range. Complete details of the test procedures, including specimen preparation, and types of measuring devices and data monitoring techniques used, are reported elsewhere (Ref. 5).

Static Test Results

Eleven specimens were tested in the static test investigation. The geometric properties that were varied in the parametric study included: the depth of the beam sections (W14x38 and W8x21), the thickness and length of the beam flange angles, the gage and spacing of the bolts in the leg of the flange angles connected to the column flange, and the thickness and length of the web angles.

Details of the connection geometries are reported in Table 1; a summary of the results is presented in Table 2. Table 2 contains the initial stiffness of the connection (initial slope of the moment-rotation curve); the slope and intercept moment of a secant line from the origin and intersecting the moment-rotation ($M-\phi$) curve at a rotation of $4x10^{-3}$ radians, and the tangent slope to the $M-\phi$ curve at $24x10^{-3}$ radians. The latter slope, although not intended to indicate a constant or final slope for a specific connection, does allow comparisons to be made among the various connections, as well as quantifying the degree of softening of a connection relative to its initial stiffness. Similarly, the secant slope offers an additional indication of the early stiffness of the connection. In some respects, the secant slope may be more representative than the initial tangent slope, because the latter is highly sensitive to irregularities (fit-up adjustments, etc.) in the early stage of loading.

The complete moment-rotation curves for several of the connections are shown in Figs. 4-7. In all of the static tests, the connections exhibited an $M-\phi$ response that became non-linear early in the loading. This is attributed, primarily, to local yielding and eventual plastic hinge formation at each toe of the fillet in the angle attached to the tension flange of the beam. Another hinge developed in the vicinity of the bolt line on the leg of the flange angle attached to the column, together with progressive plastic hinging in the outstanding legs of the web angles. Specimens 8S2 and 14S2 exhibited slip in the connection angles during testing; these were the stiffer connections for each beam size, developing the larger moments (and larger bolt shear forces) in each test group. (In a subsequent investigation, 7/8-in. diameter bolts are

TABLE 1
SCHEDULE OF TEST SPECIMENS

Specimen Number	Type of Test	Beam Section	Top and Bottom Flange Angles				Web Angles	
			Angle	Length (inches)	Gage in Leg on Column Flange (inches)	Bolt Spacing in Leg on Column Flange (inches)	Angle	Length (inches)
14S1	Static	W14X38	L6X4X3/8	8	2½	5½	2L4X3½X¼	8½
14S2	Static	W14X38	L6X4X½	8	2½	5½	2L4X3½X¼	8½
14S3	Static	W14X38	L6X4X3/8	8	2½	5½	2L4X3½X¼	5½†
14S4	Static	W14X38	L6X3½X3/8	8	2½	5½	2L4X3½X3/8	8½
8S1	Static	W8X21	L6X3½X5/16	6	2	3½	2L4X3½X¼	5½
8S2	Static	W8X21	L6X3½X3/8	6	2	3½	2L4X3½X¼	5½
8S3	Static	W8X21	L6X3½X5/16	8	2	3½	2L4X3½X¼	5½
8S4	Static	W8X21	L6X6X3/8	6	4½	3½	2L4X3½X¼	5½
8S5	Static	W8X21	L6X4X3/8	8	2½	5½	2L4X3½X¼	5½
8S6	Static	W8X21	L6X4X5/16	6	2½	3½	2L4X3½X¼	5½
8S7	Static	W8X21	L6X4X3/8	6	2½	3½	2L4X3½X¼	5½
14C1	Cyclic	W14X38	L6X4X3/8	8	2½	5½	2L4X3½X¼	8½
14C2	Cyclic	W14X38	L6X4X½	8	2½	5½	2L4X3½X¼	8½
8C1	Cyclic	W8X21	L6X3½X5/16	6	2	3½	2L4X3½X¼	5½
8C2	Cyclic	W8X21	L6X3½X3/8	6	2	3½	2L4X3½X¼	5½

†Two bolts at 3-inch spacing, mounted in top two holes on stub column, Figure 1.

TABLE 2
SUMMARY OF STATIC TEST RESULTS

Specimen Number	Initial Slope of M-ϕ Curve (k-in./radian)	Slope of Secant Line to M-ϕ Curve at $4X10^{-3}$ radians (k-in./radian)	Moment at $4X10^{-3}$ radians (k-in.)	Slope of M-ϕ Curve at $24X10^{-3}$ radians (k-in./radian)	Moment at $24X10^{-3}$ radians (k-in.)	Remarks
14S1	$195.0X10^{+3}$	$108.7X10^{+3}$	435	$5.8X10^{+3}$	668	
14S2	295.0	151.8	607	12.6	(947)	Major slip at $12X10^{-3}$, $20X10^{-3}$ radians
14S3	115.9	88.8	355	7.2	652	
14S4	221.9	124.0	496	8.3	822	
8S1	66.7	44.3	177	4.1	329	
8S2	123.4	69.0	276	1.5	(384)	Major slip at $16X10^{-3}$ radians
8S3	104.7	64.3	257	4.0	422	
8S4	15.3	14.4	57.5	2.2	165	
8S5	76.7	47.9	191.5	2.7	337	
8S6	39.5	30.0	120	3.2	244	
8S7	48.0	40.8	163	3.2	381	

being used in the heavier connections to obviate or delay the occurrence of slip during testing).

The static tests have shown that, of the geometric parameters studied, those that most significantly affected the initial stiffness and static moment-rotation performance of the connections were: the depth of the beam section to which the connections were framed; the thickness of the flange angles; and the gage in the leg of the flange angle attached to the column. Although not considered in this study, an increase in bolt diameter would be expected to affect connection response, at least initially, in a manner similar to the effect of decreasing the angle gage. Variations in the length of the flange angles, and in the length and thickness of the web angles, had a less pronounced effect on

connection response than the other factors. Analytical models to predict the initial stiffness and complete M-ϕ behavior of the connections are being developed, and will be refined as additional data become available.

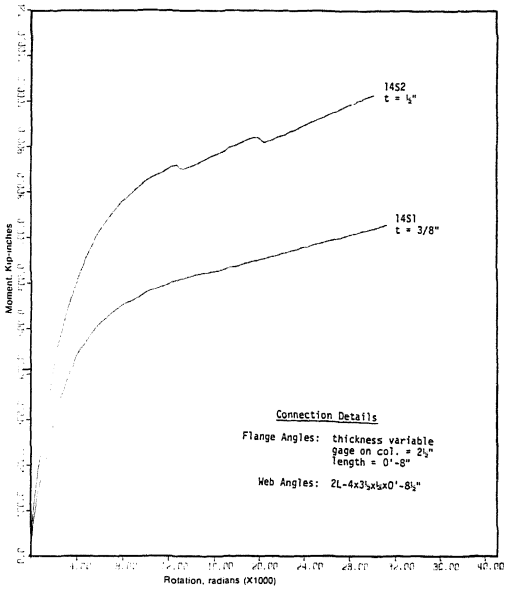

FIG. 4 EFFECT OF FLANGE ANGLE THICKNESS ON STATIC MOMENT-ROTATION BEHAVIOR — W14X38 BEAM CONNECTION

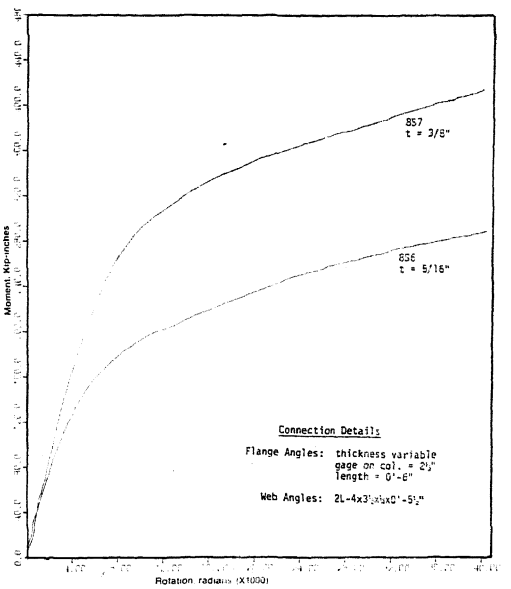

FIG. 5 EFFECT OF FLANGE ANGLE THICKNESS ON STATIC MOMENT-ROTATION BEHAVIOR — W8X21 BEAM CONNECTION

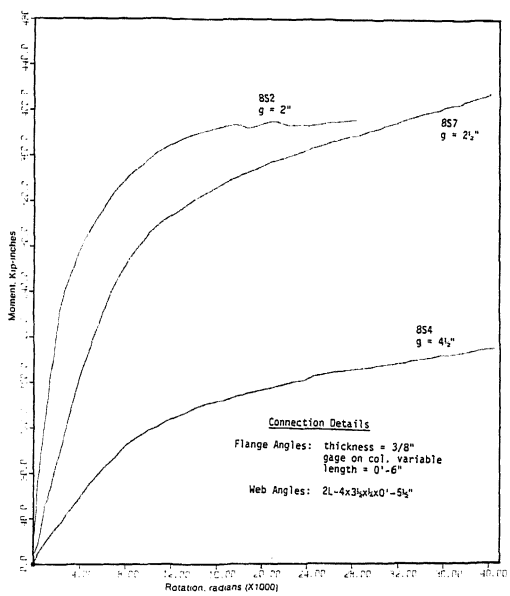

FIG. 6 EFFECT OF FLANGE ANGLE GAGE ON STATIC MOMENT-ROTATION BEHAVIOR — W8X21 BEAM CONNECTION

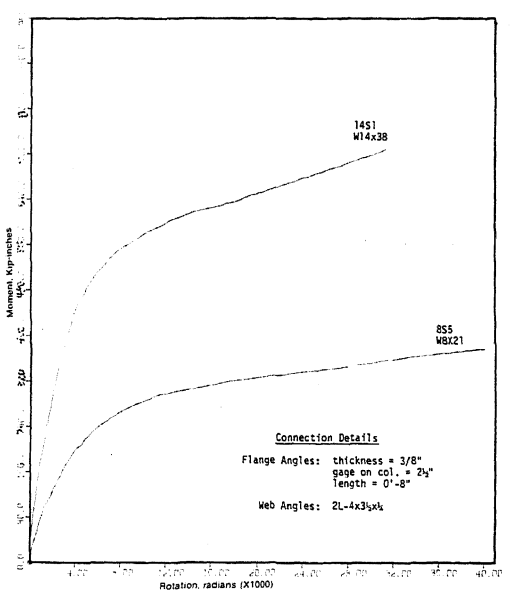

FIG. 7 COMPARISON OF STATIC MOMENT-ROTATION BEHAVIOR OF W14X38 and W8X21 BEAM CONNECTIONS

Cyclic Test Results

Four specimens were tested under cyclic loading. Two of the specimens were framed to the W14x38 beam sections, the other two framed to the W8x21 beams. For each of the beam sizes, two thicknesses of the top and seat flange angles were tested. Details of the specimen geometries are reported in Table 1. The tests were conducted using full reversal of controlled displacement. The procedure consisted of cycling sinusoidally between progressively increasing limits of displacement using the block loading pattern detailed earlier. A summary of the test results is presented in Table 3; the table includes the number of cycles applied at each amplitude, and the average range of moment and average area of one hysteresis loop recorded at each amplitude. The complete hysteresis loop traces at each test amplitude for two of the cyclic test specimens, 14C1 and 8C2, are shown in Figs. 8 and 9, respectively.

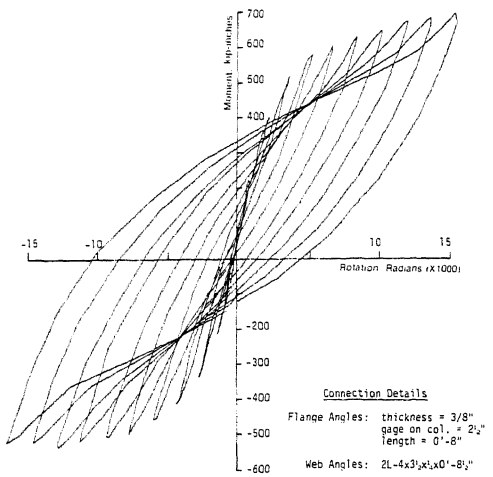

FIG. 8 STABLE HYSTERESIS LOOPS FOR SPECIMEN 14C1

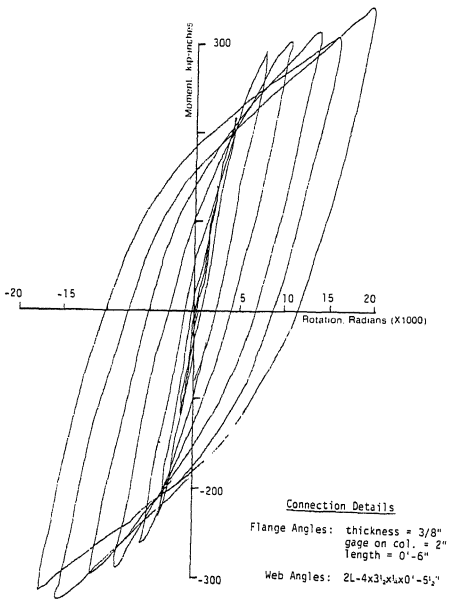

FIG. 9 STABLE HYSTERESIS LOOPS FOR SPECIMEN 8C2

Stable hysteresis loops were established, for the 14-in. test specimens, within a few cycles after an increase in amplitude was imposed relative to the preceding displacement under the block-type loading. For the 8-in. deep connections, a continual, though small, softening (loss of moment) was noted for each progressive cycle at a constant displacement amplitude; however, the hysteresis loops were otherwise similar in appearance. For each of the four specimens, the M-ϕ behavior was characterized by loops of continually decreasing slope for relatively small displacements in the non-linear range. In contrast, the hysteresis loops exhibited a "pinching" effect at larger amplitudes, the degree of pinching being more pronounced in the W14x38 beam connections than in the W8x21 members. This increase in stiffness observed toward the tip of each hysteresis loop may be attributed, in large measure, to the changing geometry of the connection during each half cycle of loading. As rotation pro-

TABLE 3
SUMMARY OF CYCLIC TEST RESULTS

Actuator Displacement Range (inches)	Cyclic Freq. (Hz)	Specimen 14C1			Specimen 14C2			Specimen 8C1			Specimen 8C2		
		No. of Cycles	Average Range of Moment (k.-in.)	Average Hysteresis Loop Area (k.-in.)	No. of Cycles	Average Range of Moment (k.-in.)	Average Hysteresis Loop Area (k.-in.)	No. of Cycles (k.-in.)	Average Range of Moment (k.-in.)	Average Hysteresis Loop Area (k.-in.)	No. of Cycles	Average Range of Moment (k.-in.)	Average Hysteresis Loop Area (k.-in.)
0.4	0.5	4	*	*	0	--	--	0	--	--	0	--	--
	.1	3	438.7	0	1	472.3	0	1	231.2	.045	1	252.2	.062
	.25	0	--	--	12	486.6	0	10	233.8	.037	10	268.9	.317
	.5	11	438.2	0	0	--	--	0	--	--	0	--	--
0.8	.1	3	741.7	.177	1	850.7	.238	2	397.3	.309	2	446.7	.381
	.25	12	749.7	.069	12	844.1**	.200**	10	422.2	.162	10	453.8	.254
1.2	.1	3	933.1	.491	1	1132	.725	3	489.9	.927	2	560.2	1.355
	.25	12	930.7	.282	12	1152	.313	10	484.0	.774	10	554.5	1.265
1.6	.1	3	1048	1.143	3	1349	1.128	4	514.6	2.340	3	598.8	3.012
	.25	12	1041	.828	12	1332	.906	10	490.1	2.361	10	592.9	2.903
2.0	.1	3	1116	2.08	1	1490	2.809	4	502.4	4.249	2	617.7	5.21
	.25	12	1106	1.79	12	1466	2.222	10	499.7	4.283	10	611.1	4.956
2.4	.1	3	1158	3.50	1	1571	4.563	2	517.6	6.225	2	636.1	7.284
	.25	12	1140	3.20	12	1537	4.038	10	493.1	6.061	10	650.2	7.063
2.8***	.1	3	1188	5.31	5	1582	6.086	2	488.4	7.775	2	661.4	9.676
	.25	12	1170	4.99	12	1568	6.27				2	653.2	9.449
3.2	.1	4	1249	6.74	2	1638	8.501						
	.25	12	1217	6.52	12	1607	8.594						
3.6	.1	3	1235	8.88	1	1670	11.487						
	.25	12	1206	8.45	12	1634	10.848						
4.0	.1	3	1234	10.88	4	1653	13.789						
	.25	8	1197	10.32									

* Data not recorded

** Data questionable

*** For Specimen 14C2, two additional cycles were imposed at 1.0in. displacement range, 0.1 Hz. Avg. range of moment: 661.2 k.-in.; avg. hysteresis loop area: 0.343 k.-in.

gresses, following a reversal in the direction of the moment at the connection, there is a period when both flange angles are drawn away from the column. With the connection in this configuration, the slope of the moment-rotation curve decreases as rotation proceeds. Eventually, the vertical leg of the compression flange angle folds back into full bearing on the column, with the connection exhibiting a concurrent increase in relative stiffness (pinching of the M-ϕ curve).

Each of the cyclic tests culminated in the formation and subsequent propagation of fatigue cracks at the toe of the fillet in one or more of the beam flange angles. The tests were terminated when cracking had progressed at least partially across the face of the angle at the fillet; no tests were extended to the point of rupture of a connection element. The connections maintained ductile behavior during the full extent of the cyclic tests, and exhibited only modest loss of maximum moment from the time fatigue cracking was noticed to the termination of the test. No slip was observed during the cyclic tests, nor was there any local buckling of the connection elements.

The block-type cyclic tests demonstrated the stability of the connections studied under large amplitude displacements, and enabled quantification of their cyclic energy absorption capacities. The tests have shown, also, that unless general frame instability intervenes under multiple excursions of lateral displacement typical of seismic loading, the effectiveness of connections of the type studied herein may be limited by low cycle fatigue of the connection elements. Additional data are needed with which to assess the accumulation of fatigue damage in these connections; this is to be addressed in a subsequent investigation.

REFERENCES

1. Beam-to-Column Building Connections: State of the Art, Preprint 80-179, American Society of Civil Engineers Annual Convention and Exposition, Portland, Oregon, April 14-18, 1980.

2. Proceedings, 4th World Conference on Earthquake Engineering, Vol. II, Santiago de Chile, January, 1969.

3. "Type 2 Construction with Wind Moment Connections: A Return to Simplicity," American Iron and Steel Institute, Washington, D.C., 1976.

4. Frye, M.J., and Morris, G.A., "Analysis of Flexibly-Connected Steel Frames," Canadian Journal of Civil Engineering, Vol. 2, 1975.

5. Altman, W.G., Jr., Azizinamini, A., Bradburn, J.H., and Radziminski, J.B., "Moment-Rotation Characteristics of Semi-Rigid Steel Beam-Column Connections," Structural Research Studies, Department of Civil Engineering, University of South Carolina, Columbia, S.C., June, 1982.